ACSNANO
www.acsnano.org
ARTICLE

Bound Layers "Cloak" Nanoparticles in Strongly Interacting Polymer Nanocomposites

Francis W. Starr,*[,†,‡] Jack F. Douglas,[¶] Dong Meng,[§] and Sanat K. Kumar[§]

[†]Department of Physics, Wesleyan University, Middletown, Connecticut 06459, United States
[‡]Department of Molecular Biology & Biochemistry, Wesleyan University, Middletown, Connecticut 06459, United States
[¶]Materials Science and Engineering Division, National Institute of Standards and Technology, Gaithersburg, Maryland 20899, United States
[§]Department of Chemical Engineering, Columbia University, New York, New York 10027, United States

ABSTRACT: **Polymer–nanoparticle (NP) interfacial interactions are expected to strongly influence the properties of nanocomposites, but surprisingly, experiments often report small or no changes in the glass transition temperature, T_g. To understand this paradoxical situation, we simulate nanocomposites over a broad range of polymer–NP interaction strengths, ε. When ε is stronger than the polymer–polymer interaction, a distinct relaxation that is slower than the main α-relaxation emerges, arising from an adsorbed "bound" polymer layer near the NP surface. This bound layer "cloaks" the NPs, so that the dynamics of the matrix polymer are largely unaffected. Consequently, T_g defined from the temperature dependence of the routinely measured thermodynamics or the polymer matrix relaxation is nearly independent of ε, in accord with many experiments. Apparently, quasi-thermodynamic measurements do not reliably reflect dynamical changes in the bound layer, which alter the overall composite dynamics. These findings clarify the relation between quasi-thermodynamic T_g measurements and nanocomposite dynamics, and should also apply to thin polymer films.**

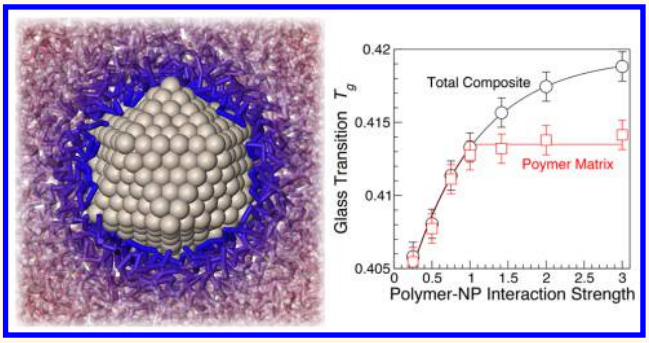

KEYWORDS: *polymer nanocomposite, glass transition, interfacial dynamics, bound polymer*

The influence of geometric confinement on the glass transition temperature (T_g) of small molecules and polymers has been intensively investigated and discussed.[1−7] The prevailing view is that surface interactions play a critical role in determining the sign and magnitude of the shift in T_g due to geometrical confinement or effective confinement through the addition of nanoparticles (NP). In particular, strong, favorable interactions are thought to increase T_g, while weak or unfavorable interactions decrease T_g. Support for this picture comes from molecular simulations showing that T_g should increase as the attractive polymer–surface interactions become stronger.[8−13] On the other hand, a number of recent experimental investigations report negligible changes in T_g in polymer nanocomposites (PNCs), even when the polymer–NP interaction is so strong that a large shift might be expected.[14−16] For example, Kumar and co-workers[5,17,18] found that the T_g of three different polymers were essentially unaffected by the presence of varying amounts of strongly interacting silica NPs. Sokolov and co-workers[19,20] confirmed these findings, and their results suggest that surface chains relax on a time scale that can be several orders of magnitude slower than the bulk chains. Indeed, in the limit of strongly favorable polymer–NP interactions, experimental measurements indicate the presence of an interfacial polymer layer with a substantially slower relaxation.[18,21−24] In the limit of irreversible adsorption, it has been suggested that the T_g changes can be related to the amount of adsorbed polymer.[25] The precise role of this "bound" layer on nanocomposite dynamics, often quantified by T_g, remains unclear.

Here, we investigate the conditions under which a distinct interfacial bound layer appears, how it is manifest in the nanocomposite equilibrium relaxation, and how it impacts thermodynamic and dynamic methods to define T_g, which sometimes decouple under confinement.[26] We find that when the polymer–NP interaction strength ε exceeds the polymer–polymer interaction strength, a distinct relaxation at very large time develops associated with the interfacial bound polymer. The NPs effectively "cloak" themselves in this bound layer, making standard quasi-thermodynamic and dynamic estimates of T_g, which primarily weight the matrix chains, insensitive to ε.

Received: August 23, 2016
Accepted: November 29, 2016
Published: November 29, 2016

DOI: 10.1021/acsnano.6b05683
ACS Nano 2016, 10, 10960–10965

The bound chains also affect the overall relaxation of the nanocomposite, but care is required to to separate the matrix and bound components of the relaxation. These results demonstrate that, while the dynamics of the nanocomposites are indeed greatly altered by strongly interacting NPs, commonly employed T_g measurements often do not reflect these changes because the matrix and the interfacial dynamics effectively decouple.

RESULTS AND DISCUSSION

Our results are based on coarse-grained molecular simulations of an icosahedral NP with variable polymer−NP interaction strength in a dense melt of unentangled polymer chains of 20 monomers in length; the behavior of this model has been described in several earlier studies.[10,27,28] In real units, the NP diameter maps to ≈15 nm, and the loading fraction is ≈5%. The Methods section and refs 10 and 28 provide further technical details.

We first characterize the spatial variation of composite dynamics *via* the time dependence of the self-intermediate scattering function,

$$F_s(q, t) = \frac{1}{N}\left\langle \sum_{j=0}^{N} e^{i\mathbf{q}\cdot(\mathbf{r}_j(t)-\mathbf{r}_j(0))} \right\rangle \quad (1)$$

at a q value corresponding to the structure factor maximum. To study the dependence of relaxation on distance from the NP, we separate $F_s(q, t)$ into "layers" of thickness 0.5σ (where σ is monomer diameter), based on monomer distance from the NP. Figure 1a,b shows the expected behavior for the distance dependence of the relaxation of $F_s(q, t)$; namely, polymer relaxation near the NP surface is substantially enhanced for weak NP−polymer interactions or substantially slowed for strong interactions. The full time dependence in each layer can be described by

$$F_s(q, t) = (1 - A)\, e^{-(t/\tau_v)^{3/2}} + A\, e^{(-t/\tau_\alpha)^{\beta}} \quad (2)$$

where the short vibrational relaxation time scale, $\tau_v = 0.29$, can be taken as a constant over the entire range of data; the $t^{3/2}$ dependence of the vibrational relaxation results from a Gaussian approximation to $F_s(q, t)$ with displacements that are intermediate between ballistic and Brownian motion, consistent with fractional Brownian motion.[29] Figure 1c shows the resulting distance dependent relaxation time, $\tau_\alpha(d)$, for a wide range of ε values. The relaxation time nearest the NP interface varies by more than 5 orders of magnitude over the ε range studied, which can be understood in terms of an alteration of the local free-energy barrier for relaxation. There is a crossover between enhanced and slowed surface relaxation that occurs for $0.5 < \varepsilon < 0.75$ (Figure 1c, inset), similar to the case of thin films.[11] In this range of ε, the NP has almost no effect on dynamics, suggesting a cancelation of enthalpic effects (favorable polymer−NP interactions) and the entropic penalty associated with the decrease of the number of available chain conformations near the surface. The relaxation behavior at large ε is consistent with the notion of a bound polymer layer, where the interfacial relaxation becomes much slower than the surrounding polymer matrix. In the limit of low T or large ε, these layers can even appear to be effectively irreversibly adsorbed.

We quantify the scale ξ over which this surface effect propagates *via*[30]

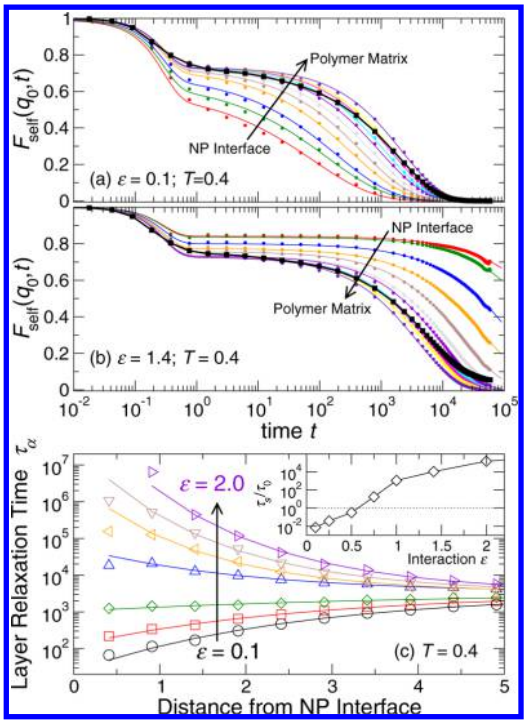

Figure 1. Self-intermediate scatting function, $F_s(q, t)$ at temperature $T = 0.4$ for polymer−NP interaction strengths (a) $\varepsilon = 0.1$ and (b) $\varepsilon = 1.4$. Symbols are simulation data, and lines are the fit defined by eq 2. The black data and line indicate $F_s(q, t)$ averaged over the entire matrix, while colored data are for layers of increasing distance from the NP surface. Note that at $\varepsilon = 1.4$, where surface relaxation is greatly diminished, the overall $F(q, t)$ has qualitatively different behavior at large t, described by eq 4. (c) The spatial variation of the relaxation time $\tau_\alpha(r)$ for (from bottom to top) $\varepsilon = 0.1$, 0.25, 0.5, 0,75, 1.0, 1.4, and 2.0 at $T = 0.4$. The effect of interaction on dynamics changes sign between $0.5 < \varepsilon < 0.75$. The distance dependence of $\tau_\alpha(d)$ is described by eq 3; the inset shows the variation in the relative surface relaxation τ_s/τ_0, so that $\tau_s/\tau_0 = 1$ defines a dynamically "neutral" interface. Note that values of $\tau_\alpha > 10^5$ are based an extrapolation of the fit (eq 2) to available data.

$$\ln \tau_\alpha(d, \varepsilon) = \ln\left[\frac{\tau_s(\varepsilon)}{\tau_0}\right] e^{-d/\xi(\varepsilon)} + \ln \tau_0 \quad (3)$$

where $d = (r - r_0)$ is the distance from the NP interface; $r_0 = a/4(1 + \sqrt{5}) = 4.54\sigma$ is the radius of the sphere that touches the middle of each icosahedral edge (and corresponds to the distance from the NP center where the monomer density first deviates from zero); τ_0 is the asymptotic value of the matrix relaxation time (which is close to that of the pure polymer melt), and $\tau_s(\varepsilon)$ is the surface relaxation time. The fit function (eq 3) is shown as solid lines in Figure 1c, from which we find that the interfacial scale $\xi(\varepsilon)$ varies weakly in the range ≈1.5−2.5σ or about 1−3 nm. Thin film experiments suggest that the size of this region may depend on whether dynamics are enhanced or diminished;[31] our results for ξ are not sufficiently precise to distinguish such an effect. Note that the dimensions of the chains in this region are not significantly altered from those of matrix chains, though the interfacial chains tend to align with the NP interface.[10]

Experimentally, the distance dependence of $F_s(q, t)$ is not readily accessible, so we consider how the substantial variations in local relaxation time are reflected in its overall behavior. Figure 2a shows the overall $F_s(q, t)$ for various ε at a

DOI: 10.1021/acsnano.6b05683
ACS Nano 2016, 10, 10960−10965

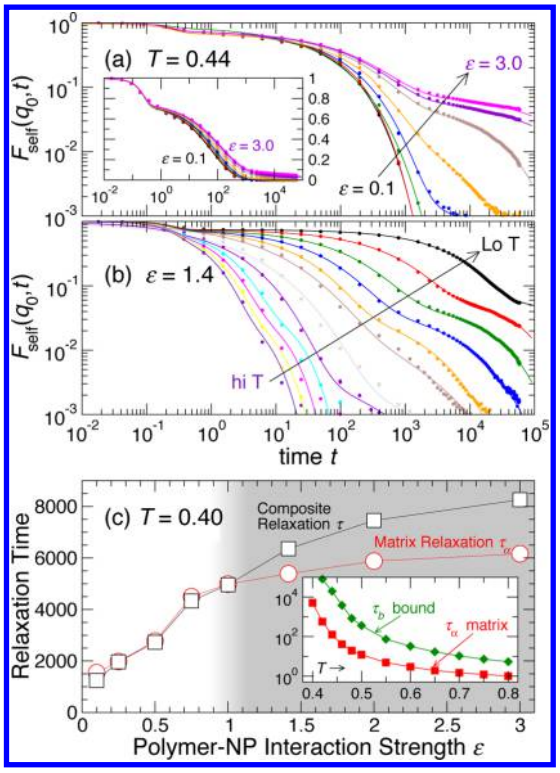

Figure 2. (a) The self-intermediate scatting function, $F_s(q_0, t)$, at T = 0.44 for polymer−NP interaction strengths (from left to right) ε = 0.1, 0.25, 0.5, 0.75, 1.0, 1.4, 2.0, and 3.0. For $\varepsilon > 1$, a distinct third relaxation emerges due to slowly relaxing "bound" chains near the NP interface. For $\varepsilon \leq 1$, the solid lines are the result of the fit to the two-step relaxation model (eq 2); for $\varepsilon > 1$, the solid lines are the result of the fit to the three-step bound polymer relaxation model (eq 4). The main panel is a log−log representation, while the inset is a log−linear representation of the same data. (b) The temperature dependence of $F_s(q_0, t)$ for ε = 1.4, where bound chains play a significant role in relaxation. From right to left, temperatures are T = 0.4, 0.42, 0.44, 0.46, 0.48, 0.5, 0.55, 0.6, 0.65, 0.7, 0.75, and 0.8. The solid lines are the result of the fit to the three-step bound polymer relaxation model (eq 4). (c) Dependence of the matrix relaxation time τ_α, and the overall composite relaxation time τ with increasing polymer−NP interaction strength, ε. These relaxation times become distinct when there is a bound layer (shaded region, $\varepsilon \gtrsim 1$). The inset shows the T dependence of the matrix, τ_α, and bound, τ_b, relaxation times for ε = 1.4.

representative T = 0.44. For $\varepsilon \gtrsim 1$, a qualitative change of behavior becomes apparent; namely, an additional relaxation process in $F_s(q, t)$ appears at large t, which is most apparent in the double-log representation. This additional relaxation process occurs due to the "bound" polymer with very slow surface relaxation that emerges at large ε. Figure 2b further shows the emergence of the bound polymer as a function of temperature for ε = 1.4. Evidence of an additional relaxation process in $F_s(q, t)$ was also found in simulations of composites with strongly interacting nanorods.[32] For cases where the bound subgroup appears, the relaxation of $F_s(q, t)$ cannot be described by the two-step relaxation of eq 2. Rather, we can describe the full t dependence of $F_s(q, t)$ by adding a third relaxation process that explicitly defines a time scale τ_b for the bound polymer relaxation,

$$F_s(q, t) = (1 - A)\, e^{-(t/\tau_v)^{3/2}} + (A - A_b)\, e^{(-t/\tau_\alpha)^{\beta}} + A_b\, e^{-(t/\tau_b)^{\beta_b}} \quad (4)$$

where $A_b = N_b/N$ defines the fraction of bound polymer. In this expression, τ_α defines the relaxation of the polymer matrix, which effectively averages over local polymer relaxation away from the substrate. Both the matrix and bound relaxation processes are described by a stretched exponential with stretching exponents β and β_b (respectively), which, at low T, are in the range 0.4−0.6. The solid lines in Figure 2 show that this three-step relaxation function can account for the relaxation over all time scales, spanning three decades of relaxation of $F_s(q, t)$. The nonergodicity parameter $A \approx 0.75$, independent of T and ε. For $\varepsilon \leq 1$, $A_b = 0$ within the precision of our results; for ε larger than the polymer−polymer interaction strength, the bound fraction, A_b, increases weakly in the range 0.05−0.075. Integrating over the monomer density profile as a function of distance from the NP, this fraction is equivalent to a bound thickness of ≈1.5−2σ, similar to the scale that emerges from the fit of eq 3 to the relaxation gradient. Consistent with experiments,[19] τ_b is typically 1−2 orders of magnitude larger than the matrix relaxation time, τ_α (inset of Figure 2b), and the difference grows with increasing ε. The presence of two structural relaxation processes, one corresponding to the surface and one to the bulk polymer, has been reported by several experiments,[19,33,34] including those on polymer films near flat surfaces. The substantial difference in the relaxation of matrix and bound polymers causes the overall composite relaxation, defined by $F_s(q,\tau) = A\, e^{-1} \approx 0.28$, to deviate from the matrix relaxation time τ_α for $\varepsilon > 1$, illustrated in Figure 2c. It is notable that the matrix relaxation becomes nearly constant for $\varepsilon > 1$, while the overall composite relaxation is modestly larger and continues to grow. Thus, T_g, as defined by a fixed relaxation time τ of the material as whole, should increase weakly with polymer−NP attraction ε, even while the matrix relaxation is nearly constant. This is the "cloaking" effect of the bound polymer, and we shall return to this point when we examine a quasi-thermodynamic T_g definition.

We did not anticipate that a continuous gradient of relaxation times (Figure 1c) should give rise to two distinct relaxation processes, though this effect was predicted theoretically.[35] To confirm consistency between the description of a continuous gradient *versus* effectively distinct relaxations, we checked that the local relaxation averaged over the matrix region (excluding the bound layer) independently recovers the matrix relaxation time τ_α obtained by fitting the overall relaxation to eq 4. In many cases, it may be difficult to measure the relaxation with sufficient precision to estimate the bound polymer thickness and relaxation. Fortunately, the separation of time scales of the bound layer can be utilized to approximate the fraction, A_b, of bound polymer (and hence its thickness) from eq 4. Specifically, if we treat the bound layer as frozen ($\tau_b \gg \tau_\alpha$), then the scattering function at the overall relaxation time τ is

$$F(q, \tau) = A\, e^{-1} \approx (A - A_b)\, e^{-(\tau/\tau_\alpha)^{\beta}} + A_b \quad (5)$$

where we drop the first term of eq 4 for the fast relaxation, which is essentially zero at time τ. A_b can then be obtained by rearrangement of this expression, which yields

$$A_b = A\frac{e^{1-(\tau/\tau_\alpha)^{\beta}} - 1}{e^{1-(\tau/\tau_\alpha)^{\beta}} - e} \approx \frac{A}{e - 1}\left[\left(\frac{\tau}{\tau_\alpha}\right)^{\beta} - 1\right] \quad (6)$$

DOI: 10.1021/acsnano.6b05683
ACS Nano 2016, 10, 10960−10965

where the final approximate result is obtained by expanding the exponential to first order, and is only valid assuming that $\tau \approx \tau_\alpha$ (i.e., $1 - (\tau/\tau_\alpha)^\beta \ll 1$, as is the case for our data). Perfect NP cloaking would imply that the matrix relaxation time τ_α equals that of the pure melt, which should be a good approximation when ε is very large. Thus, for strongly interacting NPs, the bound fraction can be estimated directly from the relaxation processes of the pure polymer and the composite.

Next, we wish to understand the consequences of distinct bound and matrix relaxations for commonly used thermodynamic approaches to define T_g. In Figure 3, we show the T

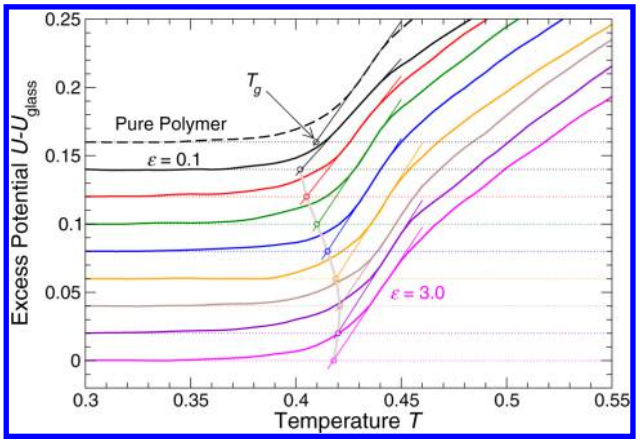

Figure 3. Excess energy, $\Delta U(T) = U(T) - U_{glass}(T)$, at fixed heating rate 10^{-5}. We define the quasi-thermodynamic rate-dependent T_g by a linear extrapolation of the vanishing of ΔU in the transition region. The circles indicate the resulting T_g values, which increase with ε and then plateau. Data are shifted vertically for clarity. From top to bottom, the curves are the pure polymer and ε = 0.1, 0.25, 0.5, 0.75, 1.0, 1.4, 2.0, and 3.0.

dependence of the excess potential energy $\Delta U(T) = U(T) - U_{glass}(T)$ on heating the glass for the range of polymer−NP interactions considered; note that we include both polymer and NP contributions to U, though only the polymer contribution is significant. Generally speaking, the measurement of T_g is complicated by the intrinsic spatial heterogeneity of the composite. Our glasses were formed by cooling at a rate of 10^{-5}, and are reheated at the same rate. It is noteworthy that these cooling rates are many orders of magnitude faster than in experiments, and correspondingly the T_g estimated is substantially higher than would be obtained at an experimental rate. Deep in the glass state ($T < 0.3$), U_{glass} is well described by a quadratic function, equivalent to a linear temperature dependence of the specific heat. Figure 3 shows that ΔU grows rapidly in the vicinity of $T \approx 0.4$ at this rate. Analogous to the experimental procedure, we define T_g by the extrapolation of a linear fit in the transition region to $\Delta U \to 0$. T_g defined in this way varies only weakly with polymer−NP interaction strength. We also considered alternate definitions of T_g based on deviations from liquid-like relaxation at high T or the extremum in specific heat; all these definitions show the same qualitative increase and saturation of T_g at large ε.

We are now in a position to contrast the behavior of T_g from thermodynamic and dynamic definitions (Figure 4). Dynamically, T_g is commonly defined by a fixed relaxation time that corresponds roughly to accessible cooling and heating rates, and experimentally this is typically 100 s. Since our thermodynamic definition of T_g corresponds to a much faster

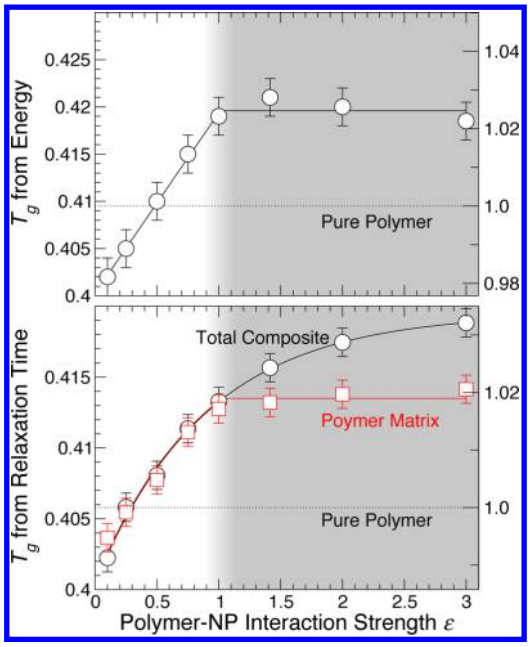

Figure 4. (a) T_g defined from thermodynamics in Figure 3; T_g defined in this way plateaus when bound polymer emerges (shaded region). (b) Dynamical definition of T_g, namely, $\tau(T_g) = 10^3$. Black symbols define T_g for the overall composite relaxation, τ, while red symbols define T_g from the matrix component of relaxation, τ_α. Like the thermodynamic T_g, the matrix component plateaus when bound polymer develops. The right-hand axis indicates T_g normalized by the corresponding bulk material, highlighting the small amplitude of T_g changes.

cooling rate than experiments, we correspondingly define the dynamic T_g by a shorter time scale, specifically as the temperature where $\tau = 10^3$ (in LJ units); our findings do not change qualitatively if we choose a larger time scale. There are multiple implications raised by the T_g results. First, the T_g from the quasi-thermodynamic definition is essentially independent of polymer−NP interaction strength for $\varepsilon \gtrsim 1.0$ (i.e., greater than polymer−polymer interaction strength). In parallel, the behavior of T_g defined from the relaxation of the matrix τ_α also shows saturation for $\varepsilon \gtrsim 1.0$. Indeed, Figures 1 and 2 confirm that this is precisely the region where a distinct bound polymer relaxation develops. Thus, the saturation of T_g is a consequence of the bound polymer layer cloaking the effects of NP interactions. On the other hand, T_g defined by the overall composite relaxation τ (that includes bound chains) increases monotonically with increasing ε. Apparently, the thermodynamic definition of T_g is insensitive to the very slowly relaxing bound polymer and only reflects the dynamics of the matrix polymer. Naively, one might expect linear growth of T_g from the overall composite dynamics with increasing ε; however, the overall dynamical T_g increases sublinearly when bound polymer develops, since the effect of NP interactions on matrix chains is cloaked. As a result, even for strong polymer−NP interactions, the effect on any of these measures of T_g is $\lesssim$5%. Even for larger NP loading fractions (when the fraction of bound polymer must be proportionally larger), the effect on T_g defined by thermodynamic variations or matrix chain dynamics will be small due to cloaking, consistent with experiments. We have confirmed this effect in simulations at twice the NP concentration of the present data (not shown). The weak T_g

DOI: 10.1021/acsnano.6b05683
ACS Nano 2016, 10, 10960−10965

dependence is generally a consequence of the fact that the bulk relaxation decouples from the surface, which is nearly "frozen".

CONCLUSIONS

Our results show that is possible to explicitly define a distinct fraction of bound polymer with specified relaxation time. In doing so, we show that typical thermodynamic and dynamic measures of T_g, which focus on the temperature dependence of the dominant fraction of relaxing chains, do not capture the signatures of much slower, strongly interacting surface chains, and hence yield T_g estimates that are effectively only sensitive to the bulk-like polymer matrix relaxations. While we have focused on distinct relaxation due to slowly relaxing chains, it is possible to have a distinct relaxation due to rapidly relaxing chains at an interface, such as occurs in freely standing thin films.[36] As a practical matter, a distinct relaxation due to a rapidly relaxing interface is more challenging to observe, unless the interfacial relaxation is enhanced by many orders of magnitude relative to the interior. In order to see surface effects beyond the dominant fraction of matrix polymers, the analysis of experimental data needs to carefully consider the distribution of relaxation times and corresponding T_g values. For example, recent NMR and dielectric measurements reveal dynamics of both interfacial and bulk-like polymer.[37,38] These efforts hold the promise to more clearly identify the signatures of the bound polymer layer that forms near the NP surface, or in supported polymer films.

METHODS

Our findings are based on molecular dynamics simulations of a polymer–NP composite examined in several earlier studies.[10,27,28] Polymer chains are represented by the Kremer–Grest bead–spring model,[39] in which nonbonded beads interact *via* a Lennard-Jones (LJ) potential of strength, ε_p, truncated at 2.5 times the bead diameter, σ, to include attractive interactions; bonded beads are connected by a finitely extensible nonlinear elastic (FENE) potential. We consider chains of length 20 beads, below the entanglement molecular mass. A collection of 356 LJ particles are bonded together to form a large icosahedral NP. The outer shell of the icosahedron has 6 LJ particles along the edges, with edge length $a = 5.61\sigma$, similar to the chain end-to-end distance. Additional details of the model and simulation parameters can be found in ref 28. We use reduced units where $\varepsilon_p = \sigma = 1$, though the reduced units can be mapped to physical units relevant to typical polymer materials where $\sigma \approx 1$ nm, time is measured in picoseconds, $\varepsilon_p \approx 1$ kJ/mol, and $T_g \approx 100$ °C; using this conversion, the NP diameter is ≈15 nm. We employ periodic boundary conditions in all three directions using 1 NP and 400 chains, corresponding to a NP volume fraction 0.0426 (≈5% loading). All simulations are performed under isothermal–isobaric conditions with the pressure set to $P = 0.1$, resulting in simulation box sizes of 20 to 21.2, depending on temperature and polymer–NP interaction strength, ε ($0.1 \leq \varepsilon \leq 3$). We vary temperature in the range $0.4 \leq T \leq 0.8$. Each system is equilibrated for a minimum of 100 times the polymer matrix relaxation time of the incoherent (or self-intermediate) scattering function. To mimic experimental methods to measure T_g based on thermodynamic variables, we also carry out cooling and reheating simulations using a fixed rate 10^{-5}; the resulting T_g estimate is close to the lowest T of our equilibrium dynamics simulations. Results are averaged over five independent runs at each interaction strength and T.

AUTHOR INFORMATION

Corresponding Author

*E-mail: fstarr@wesleyan.edu.

ORCID

Francis W. Starr: 0000-0002-2895-6595

Notes

The authors declare no competing financial interest.

ACKNOWLEDGMENTS

Computer time was provided by Wesleyan University. This work was supported in part by NIST Award 70NANB15H282.

REFERENCES

(1) Alcoutlabi, M.; McKenna, G. B. Effects of Confinement on Material Behaviour at the Nanometre Size Scale. *J. Phys.: Condens. Matter* **2005**, *17*, R461–R524.

(2) Jackson, C. L.; McKenna, G. B. The Melting Behavior of Organic Materials Confined in Porous Solids. *J. Chem. Phys.* **1990**, *93*, 9002–9011.

(3) Keddie, J. L.; Jones, R. A. L.; Cory, R. A. Size-Dependent Depression of The Glass-Transition Temperature in Polymer-Films. *Europhys. Lett.* **1994**, *27*, 59–64.

(4) Keddie, J. L.; Jones, R. A. L.; Cory, R. A. Interface and Surface Effects on The Glass-Transition Temperature in Thin Polymer-Films. *Faraday Discuss.* **1994**, *98*, 219–230.

(5) Bansal, A.; Yang, H.; Li, C.; Cho, K.; Benicewicz, B.; Kumar, S.; Schadler, L. Quantitative Equivalence between Polymer Nanocomposites and Thin Polymer Films. *Nat. Mater.* **2005**, *4*, 693–698.

(6) Rittigstein, P.; Priestley, R. D.; Broadbelt, L. J.; Torkelson, J. M. Model Polymer Nanocomposites Provide an Understanding of Confinement Effects in Real Nanocomposites. *Nat. Mater.* **2007**, *6*, 278–282.

(7) Rittigstein, P.; Torkelson, J. M. Polymer-Nanoparticle Interfacial Interactions in Polymer Nanocomposites: Confinement Effects on Glass Transition Temperature and Suppression of Physical Aging. *J. Polym. Sci., Part B: Polym. Phys.* **2006**, *44*, 2935–2943.

(8) Fryer, D. S.; Peters, R. D.; Kim, E. J.; Tomaszewski, J. E.; de Pablo, J. J.; Nealey, P. F.; White, C. C.; Wu, W. L. Dependence of the Glass Transition Temperature of Polymer Films on Interfacial Energy and Thickness. *Macromolecules* **2001**, *34*, 5627–5634.

(9) Torres, J. A.; Nealey, P. F.; de Pablo, J. J. Molecular Simulation of Ultrathin Polymeric Films near the Glass Transition. *Phys. Rev. Lett.* **2000**, *85*, 3221–3224.

(10) Starr, F. W.; Schrøder, T. B.; Glotzer, S. C. Molecular Dynamics Simulation of a Polymer Melt with a Nanoscopic Particle. *Macromolecules* **2002**, *35*, 4481–4492.

(11) Hanakata, P. Z.; Pazmiño Betancourt, B. A.; Douglas, J. F.; Starr, F. W. A Unifying Framework to Quantify the Effects of Substrate Interactions, Stiffness, and Roughness on the Dynamics of Thin Supported Polymer Films. *J. Chem. Phys.* **2015**, *142*, 234907.

(12) Peter, S.; Meyer, H.; Baschnagel, J. Molecular Dynamics Simulations of Concentrated Polymer Solutions in Thin Film Geometry. I. Equilibrium Properties near the Glass Transition. *J. Chem. Phys.* **2009**, *131*, 014902.

(13) Merling, W. L.; Mileski, J. B.; Douglas, J. F.; Simmons, D. S. The Glass Transition of a Single Macromolecule. *Macromolecules* **2016**, *49*, 7597–7604.

(14) Rittigstein, P.; Torkelson, J. M. Polymer-Nanoparticle Interfacial Interactions in Polymer Nanocomposites: Confinement Effects on Glass Transition Temperature and Suppression of Physical Aging. *J. Polym. Sci., Part B: Polym. Phys.* **2006**, *44*, 2935–2943.

(15) Lu, H.; Nutt, S. Restricted Relaxation in Polymer Nanocomposites near the Glass Transition. *Macromolecules* **2003**, *36*, 4010–4016.

(16) Ash, B.; Schadler, L.; Siegel, R. Glass Transition Behavior of Alumina/Polymethylmethacrylate Nanocomposites. *Mater. Lett.* **2002**, *55*, 83–87.

(17) Moll, J.; Kumar, S. K. Glass Transitions in Highly Attractive Highly Filled Polymer Nanocomposites. *Macromolecules* **2012**, *45*, 1131–1135.

(18) Harton, S. E.; Kumar, S. K.; Yang, H.; Koga, T.; Hicks, K.; Lee, E.; Mijovic, J.; Liu, M.; Vallery, R. S.; Gidley, D. W. Immobilized

DOI: 10.1021/acsnano.6b05683
ACS Nano 2016, 10, 10960–10965

Polymer Layers on Spherical Nanoparticles. *Macromolecules* **2010**, *43*, 3415−3421.
(19) Holt, A. P.; Griffin, P. J.; Bocharova, V.; Agapov, A. L.; Imel, A. E.; Dadmun, M. D.; Sangoro, J. R.; Sokolov, A. P. Dynamics at the Polymer/Nanoparticle Interface in Poly(2-vinylpyridine)/Silica Nanocomposites. *Macromolecules* **2014**, *47*, 1837−1843.
(20) Holt, A. P.; Sangoro, J. R.; Wang, Y.; Agapov, A. L.; Sokolov, A. P. Chain and Segmental Dynamics of Poly(2-vinylpyridine) Nanocomposites. *Macromolecules* **2013**, *46*, 4168−4173.
(21) Yu, C.; Granick, S. Revisiting Polymer Surface Diffusion in the Extreme Case of Strong Adsorption. *Langmuir* **2014**, *30*, 14538−14544.
(22) Jouault, N.; Moll, J. F.; Meng, D.; Windsor, K.; Ramcharan, S.; Kearney, C.; Kumar, S. K. Bound Polymer Layer in Nanocomposites. *ACS Macro Lett.* **2013**, *2*, 371−374.
(23) Sargsyan, A.; Tonoyan, A.; Davtyan, S.; Schick, C. The Amount of Immobilized Polymer in PMMA SiO_2 Nanocomposites Determined from Calorimetric Data. *Eur. Polym. J.* **2007**, *43*, 3113−3127.
(24) Napolitano, S.; Wubbenhorst, M. Dielectric Signature of a Dead Layer in Ultrathin Films of a Nonpolar Polymer. *J. Phys. Chem. B* **2007**, *111*, 9197−9199.
(25) Burroughs, M. J.; Napolitano, S.; Cangialosi, D.; Priestley, R. D. Direct Measurement of Glass Transition Temperature in Exposed and Buried Adsorbed Polymer Nanolayers. *Macromolecules* **2016**, *49*, 4647−4655.
(26) Priestley, R. D.; Cangialosi, D.; Napolitano, S. On the Equivalence between the Thermodynamic and Dynamic Measurements of the Glass Transition in Confined Polymers. *J. Non-Cryst. Solids* **2015**, *407*, 288−295.
(27) Starr, F. W.; Douglas, J. F. Modifying Fragility and Collective Motion in Polymer Melts with Nanoparticles. *Phys. Rev. Lett.* **2011**, *106*, 115702.
(28) Pazmiño Betancourt, B. A.; Douglas, J. F.; Starr, F. W. Fragility and Cooperative Motion in a Glass-Forming Polymer-Nanoparticle Composite. *Soft Matter* **2013**, *9*, 241−254.
(29) Simmons, D. S.; Douglas, J. F. Nature and Interrelations of Fast Dynamic Properties in a Coarse-Grained Glass-Forming Polymer Melt. *Soft Matter* **2011**, *7*, 11010−11020.
(30) Scheidler, P.; Kob, W.; Binder, K. Cooperative Motion and Growing Length Scales in Supercooled Confined Liquids. *Europhys. Lett.* **2002**, *59*, 701.
(31) Baglay, R. R.; Roth, C. B. Communication: Experimentally Determined Profile of Local Glass Transition Temperature Across a Glassy-Rubbery Polymer Interface with a T_g Difference of 80 K. *J. Chem. Phys.* **2015**, *143*, 111101.
(32) Toepperwein, G. N.; Riggleman, R. A.; de Pablo, J. J. Dynamics and Deformation Response of Rod-Containing Nanocomposites. *Macromolecules* **2012**, *45*, 543−554.
(33) Glor, E. C.; Fakhraai, Z. Facilitation of Interfacial Dynamics in Entangled Polymer Films. *J. Chem. Phys.* **2014**, *141*, 194505.
(34) Paeng, K.; Richert, R.; Ediger, M. D. Molecular Mobility in Supported Thin Films of Polystyrene, Poly(methyl methacrylate), and Poly(2-vinyl pyridine) Probed by Dye Reorientation. *Soft Matter* **2012**, *8*, 819−826.
(35) Mirigian, S.; Schweizer, K. S. Theory of Activated Glassy Relaxation, Mobility Gradients, Surface Diffusion, and Vitrification in Free Standing Thin Films. *J. Chem. Phys.* **2015**, *143*, 244705.
(36) Paeng, K.; Swallen, S. F.; Ediger, M. D. Direct Measurement of Molecular Motion in Freestanding Polystyrene Thin Films. *J. Am. Chem. Soc.* **2011**, *133*, 8444−8447.
(37) Cheng, S.; Holt, A. P.; Wang, H.; Fan, F.; Bocharova, V.; Martin, H.; Etampawala, T.; White, B. T.; Saito, T.; Kang, N.-G.; et al. Unexpected Molecular Weight Effect in Polymer Nanocomposites. *Phys. Rev. Lett.* **2016**, *116*, 038302.
(38) Holt, A. P.; Bocharova, V.; Cheng, S.; Kisliuk, A. M.; White, B. T.; Saito, T.; Uhrig, D.; Mahalik, J. P.; Kumar, R.; Imel, A. E.; et al. Controlling Interfacial Dynamics: Covalent Bonding *versus* Physical Adsorption in Polymer Nanocomposites. *ACS Nano* **2016**, *10*, 6843−6852.
(39) Grest, G. S.; Kremer, K. Molecular Dynamics Simulation for Polymers in the Presence of a Heat Bath. *Phys. Rev. A: At., Mol., Opt. Phys.* **1986**, *33*, 3628−3631.

DOI: 10.1021/acsnano.6b05683
ACS Nano 2016, 10, 10960−10965